Received: 31 March 2021 | Revised: 25 April 2021 | Accepted: 27 April 2021

DOI: 10.1111/ijac.13785

International Journal of Applied Ceramic TECHNOLOGY

SPECIAL ISSUE ARTICLE

Manufacture and thermomechanical characterization of wet filament wound C/C-SiC composites

Martin Frieß[1] | **Muhammed Böyükbas**[2] | **Felix Vogel**[1] | **Daniel Cepli**[1] | **Oliver Schatz**[1] | **Fabia Süß**[1] | **Yuan Shi**[1]

[1]Institute of Structures and Design, German Aerospace Center (DLR), Stuttgart, Germany

[2]Institute of Space Systems, University of Stuttgart, Stuttgart, Germany

Correspondence
Martin Frieß, Institute of Structures and Design, German Aerospace Center (DLR), Pfaffenwaldring 38-40, Stuttgart D-70569, Germany.
Email: martin.friess@dlr.de

Funding information
German Ministry of Defence

Abstract

The paper presents manufacture of C/C-SiC composite materials by wet filament winding of C fibers with a water-based phenolic resin with subsequent curing via autoclave as well as pyrolysis and liquid silicon infiltration (LSI). Almost dense C/C-SiC composite materials with different winding angles ranging from ±15° to ±75° could be obtained with porosities lower than 3% and densities in the range of 2 g/cm^3. Thermomechanical characterization via tensile testing at room temperature and at 1300°C revealed higher tensile strength at elevated temperature than at room temperature. Thus, C/C-SiC material obtained by wet filament winding and LSI-processing has excellent high-temperature strength for high-temperature applications. Crack patterns during pyrolysis, microstructure after siliconization, and tensile strength strongly depend on the fiber/matrix interface strength and winding angle. Moreover, calculation tools for composites, such as classical laminate and inverse laminate theory, can be applied for structural evaluation and prediction of mechanical performance of C/C-SiC structures.

KEYWORDS

C/C-SiC, filament winding, fracture surfaces, microstructure, pyrolysis, siliconisation, tensile testing, thermomechanical characterization, winding angle

1 | INTRODUCTION

Ceramic matrix composites (CMC) are ideal candidates for applications in hot gas environment in aerospace (e.g., rocket propulsion) due to their superior properties such as high hardness, abrasion, heat, and thermal shock resistance in combination with high damage tolerance in case of excessive loading.[1–7] Due to excellent corrosion and thermal shock resistance, C/C-SiC as a promising candidate can also be applied in thermal storage applications.[8–9]

In short-term application, C-fiber-based composites, such as carbon-silicon carbide composites (C/C-SiC) developed by DLR using the well-known LSI process, are superior to other CMC materials due to their ease of manufacture, variability of raw materials, and cost. Thus, there is a huge potential for future rocket propulsion applications.[10–14] State of the art is the use of commercially available fabrics to manufacture complex shaped CMC components with low porosity in one cycle, providing moderate strength materials, or even lower performance materials based on short fibers applied on cost-efficient components where low strength can be accepted.[15–18] Characterization of C/C-SiC composites with respect to thermal and mechanical properties was investigated under different loads and are summarized in previous studies.[7,19–22]

However, for applications requiring high specific strength components of tubular shape, a new approach combining wet filament winding technique with the LSI-route to provide a cost and time efficient process is obvious but still is a real challenge for material scientists and engineers.

2 | INVESTIGATED MATERIAL AND EXPERIMENTAL PROCEDURES

2.1 | Manufacturing process

For the manufacture of C/C-SiC composite tubes as well as plates, a three-step process based on wet filament winding and LSI-processing was chosen: (1) CFRP green body shaping by wet filament winding and pressure-less curing on the mandrel, (2) pyrolysis to a porous C/C preform, and (3) densification and build-up of SiC matrix by reactive melt infiltration.

1. The manufacture of structures with rotational symmetry requiring high specific strength in main load direction, such as combustion chambers, affords the use of winding machines and fibers of high specific strength. Therefore, a wet filament cross winding process was developed using continuous T800 12k carbon fibers, which were impregnated prior to winding with a water-based phenolic resin (MF43) and wound onto a rotating mandrel (ø = 335 mm with a length of about 220 mm) in a predetermined pattern to form an interweaved regular laminate using winding angles of ±15°, ±30°, ±45°, ±60°, and ±75°, respectively. Since mechanical characterization is much easier to achieve on plate than on tubular samples, a part of the uncured winding form was cut along the rotation axis and then unrolled to a plate shape. The uncured composite preforms (tubes and plates) were then cured at 15 bar pressure and 195°C for 3 h to achieve a predetermined fiber volume content of about 60%.
2. The polymer-based CFRP green body tubes as well as plates were pyrolyzed in an inert gas atmosphere at temperatures up to 1650°C leading to a porous C/C preform. In case of tubes, graphite mandrels with shrinkage adapted diameters were used up to 900°C.

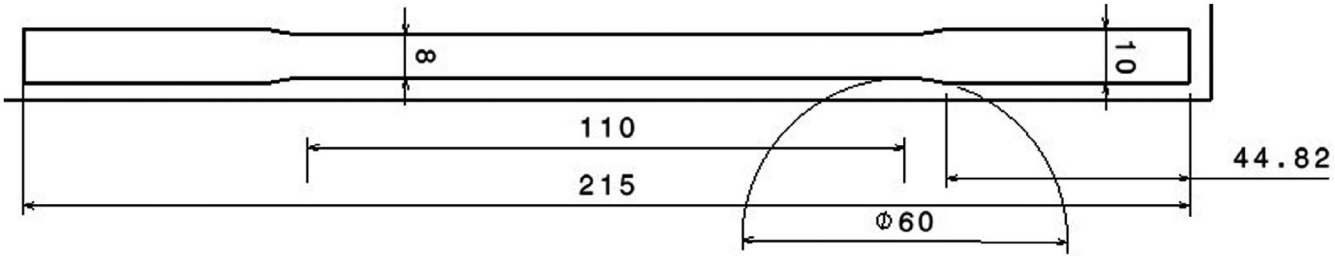

FIGURE 1 Specimen dimensions from C/C-SiC plates for tensile testing

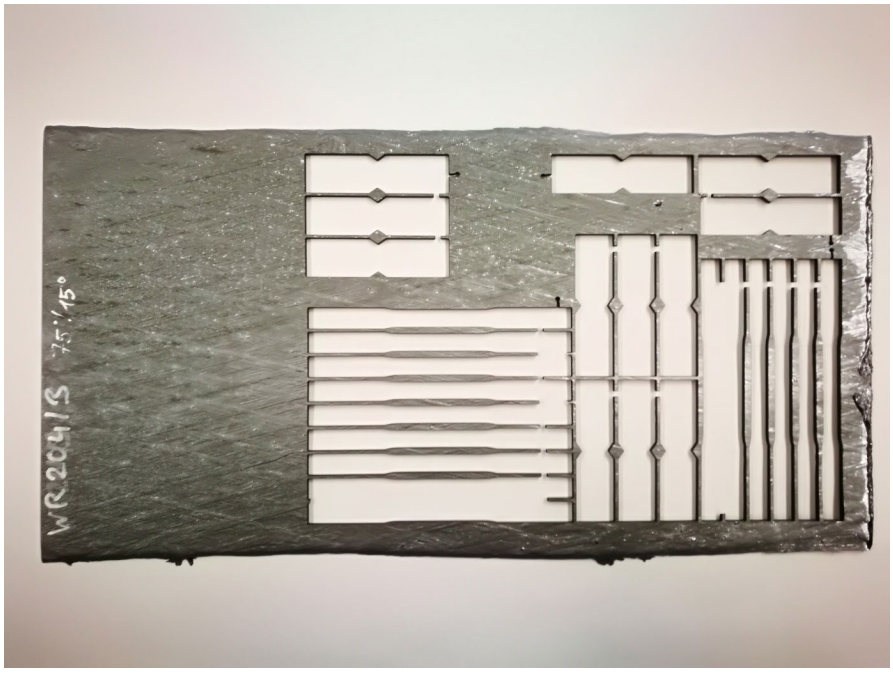

FIGURE 2 Preparation of specimens via jet-cutting from C/C-SiC plate with fiber orientation to tensile loading: ±15° (horizontal) and ±75° (vertical)

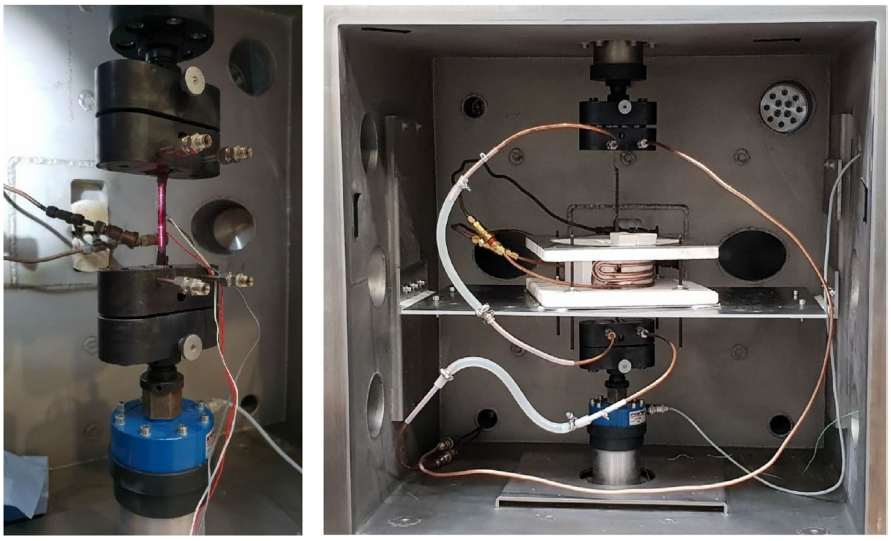

FIGURE 3 Experimental set-up in universal testing machine (Indutherm) at room temperature (left) and high temperature (right)

TABLE 1 Mechanical properties, density, and open porosity of composite plates (CFRP, C/C, and C/C-SiC) at various fibre orientations.

Fibre orient. (°)	**±15**	**±30**	**±45**	**±60**	**±75**
Plate number	WR204	WR206	WR208	WR206	WR204
Por.[a] (vol.%)	3.10	4.61	6.22	4.61	3.10
Por. (C/C) (vol.%)	15.0	14.6	15.7	14.6	15.0
Si-uptake (mass%)	34.5	38.2	40.2	38.2	34.5
T. strength (MPa)	264.9 ± 24.8	172.1 ± 20.1	58.7 ± 24.7	35.2 ± 2.6	15.7 ± 0.4
T. modulus (GPa)	137.6 ± 9.9	70.0 ± 8.4	26.9 ± 7.8	19.0 ± 3.0	22.0 ± 4.7
Fract. strain (%)	0.21 ± 0.02	0.39 ± 0.05	0.33 ± 0.14	0.55 ± 0.11	0.12 ± 0.07
Density (g/cm^3)	1.86	2.07	2.02	2.07	1.86
Porosity (%)	2.10	1.23	2.74	1.23	2.10

Abbreviations: Fract., fracture; T., tensile.

[a]CFRP state.

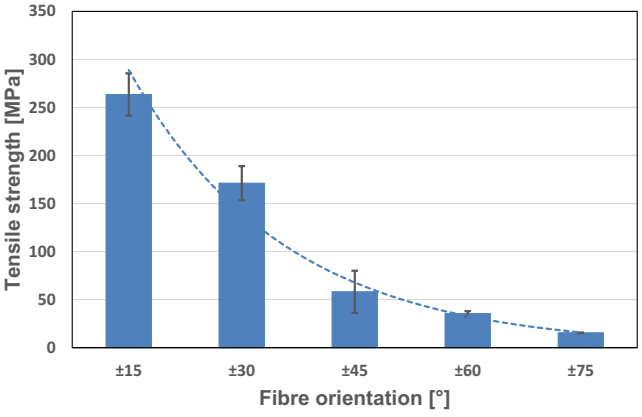

FIGURE 4 Tensile strength versus fiber orientation at room temperature showing asymptotic behavior with trendline and standard deviation

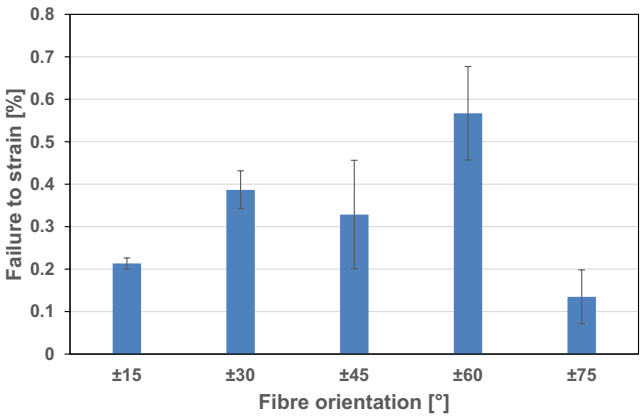

FIGURE 5 Failure to strain versus fiber orientation at room temperature with standard deviation

3. Finally, the porous, fiber reinforced preform (C/C) was infiltrated with highly pure molten silicon (semi-conductor quality) in vacuum at up to 1650°C. The molten silicon reacted with the carbon and formed the ceramic SiC matrix.

Open porosity and density were measured in all stages according to Archimedes method by immersion in demineralised water. The microstructure of the C/C-SiC composites was investigated on polished samples or on

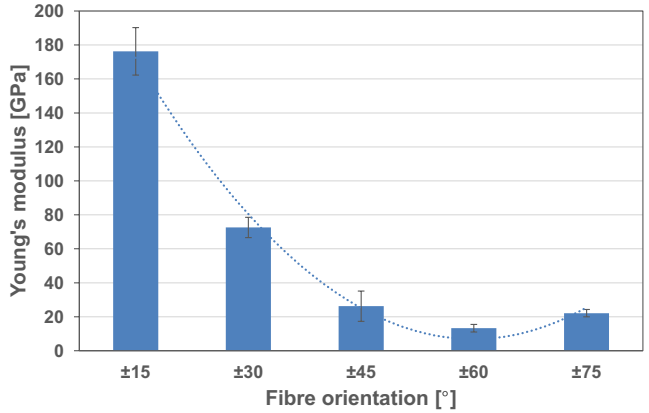

FIGURE 6 Young's modulus versus fiber orientation at room temperature showing asymptotic behavior with trendline and standard deviation

fractured surfaces by means of scanning electron microscopy (SEM, Zeiss Ultra 55) for each fiber orientation as mentioned above.

Phase analysis of tested specimens (8 mm width and about 10 mm length) in close distance to fracture area was performed by X-ray diffraction (XRD) using a 2θ-goniometer (D8 Advance, Bruker AXS) with Cu Kα radiation (154.060 pm) with a step size of 0.02° and 10 s time/step in the range of $10° < 2\theta < 90°$. In order to obtain a semi-quantitative analysis, measured areas of all tested samples were of approximately the same size. Since the amount of carbon (predominant component) and silicon carbide are determined by the LSI-process, the height of peak of carbon of all specimens was adapted to the same height by computer manipulation. The choice of silicon carbide was discarded since it is prone to height increase due to enhanced crystal growth by gas phase reactions. As silicon being present in the composite in the range of 1–2 wt% is highly dependent on testing conditions, this parameter was chosen for further investigations regarding phase composition. Crystalline Si is very sensitive to X-ray analysis, and its highest peak at about $2\theta = 28.4°$ is therefore chosen for a semi-quantitative evaluation: the higher this peak, the higher the amount of silicon in the composite.

2.2 | Procedure for specimen preparation via jet-cutting from C/C-SiC plates

Test coupons for tensile testing with dimensions (l = 215 mm, b = 10 mm, d = 3.5 mm) were obtained by

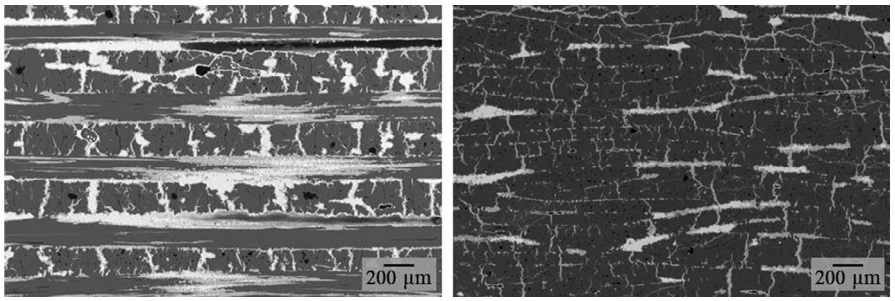

FIGURE 7 Microstructure of C/C-SiC with fiber orientation 0°/90° (left) and ±15° (right)

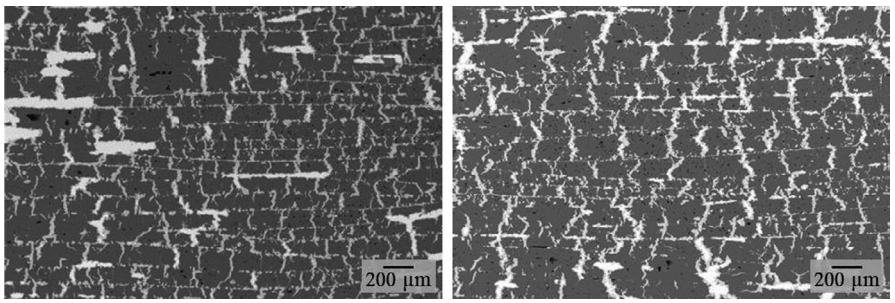

FIGURE 8 Microstructure of C/C-SiC with fiber orientation ±30° (left) and ±45° (right)

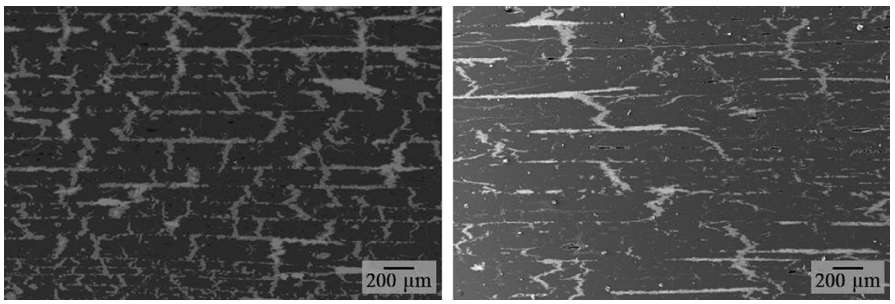

FIGURE 9 Microstructure of C/C-SiC with fiber orientation ±60° (left) and ±75° (right)

TABLE 2 Thermomechanical properties of C/C-SiC composite plates at various fiber orientations at 1300°C

Fibre orient. (°)	±15	±30	±45	±60	±75
Plate number	WR204	WR206	WR208	WR206	WR204
T. strength (MPa)	294.2 ± 12.2	238.1 ± 7.3	106.2 ± 3.9	n.d.	n.d.
T. modulus (GPa)	151.6 ± 20.6	142.2 ± 43.3	26.4 ± 0.84	n.d.	n.d.
Fracture strain (%)	0.18 ± 0.01	0.37 ± 0.03	0.75 ± 0.07	n.d.	n.d.

Abbreviations: n.d., not determined; T., tensile.

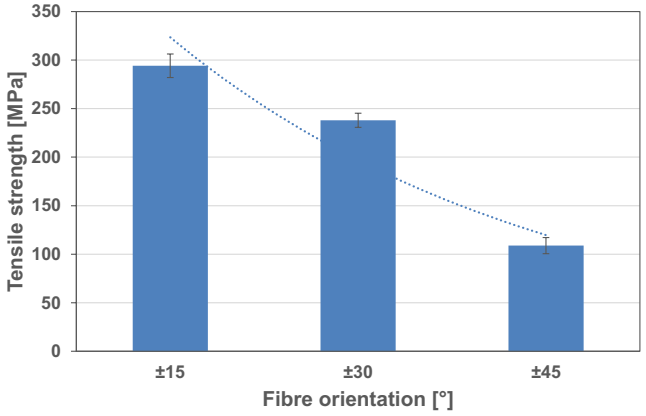

FIGURE 10 Tensile strength versus fiber orientation at high temperature (1300°C) showing asymptotic behavior with trendline and standard deviation

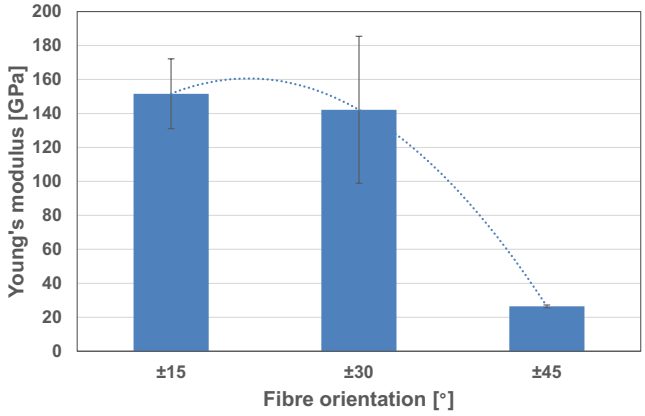

FIGURE 12 Young's modulus versus fiber orientation at high temperature (1300°C) showing asymptotic behavior with trendline and standard deviation

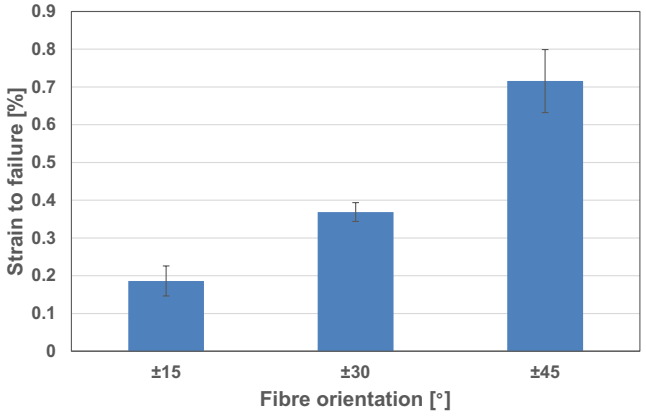

FIGURE 11 Strain to failure versus fiber orientation at high temperature (1300°C) with trendline and standard deviation

jet-cutting from C/C-SiC plates (see Figures 1 and 2 for details). Tensile testing was first performed on universal testing machine (Zwick UTS) using strain gauges for measure of elongation at room temperature. Then, for tensile testing on universal testing machine (Indutherm), strain gauges were placed on the front side and markings on the backside of the coupon in order to compare measurement of elongation at room temperature and to compare results to a laser extensometer. For high temperature, tensile testing and measurement of elongation will be performed on universal testing machine (Indutherm) applying a laser extensometer. Marking was performed by spray coating of distinct lines on specimens with Y_2O_3 particles, although different other particles (e.g., TiO_2, ZrO_2, and Al_2O_3) depending on material and testing temperature are viable.

2.3 | High temperature set-up for tensile testing of C/C-SiC plates (Indutherm)

High-temperature tensile testing and measurement of elongation will be performed on universal testing machine (Indutherm) applying a laser extensometer (Figure 3). The coupons with cold clamping and markings of alumina are heated via inductive heating at high heating rates inside isolation with alumina in nitrogen atmosphere at 1 mbar. Fast cooling of the coupons

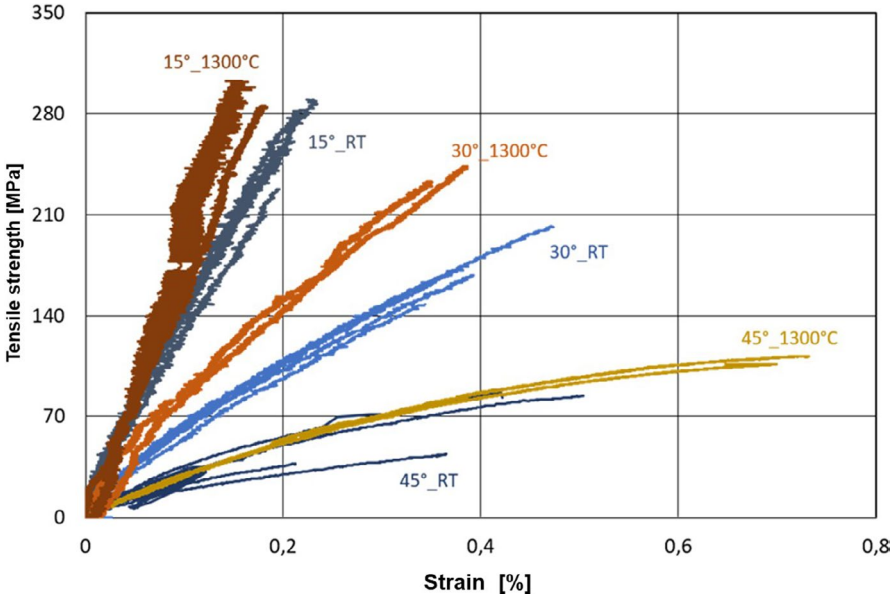

FIGURE 13 Tensile behavior versus strain at room and high temperature (1300°C)

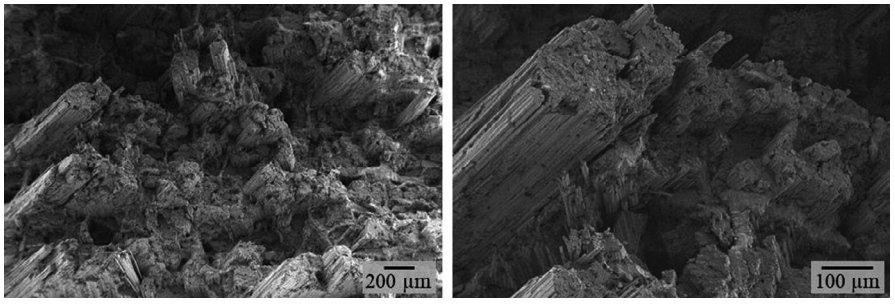

FIGURE 14 Fracture surface of C/C-SiC with fiber orientation ±15° resembling a rather high fiber pull-out (magn. 100× [left] and 350× [right])

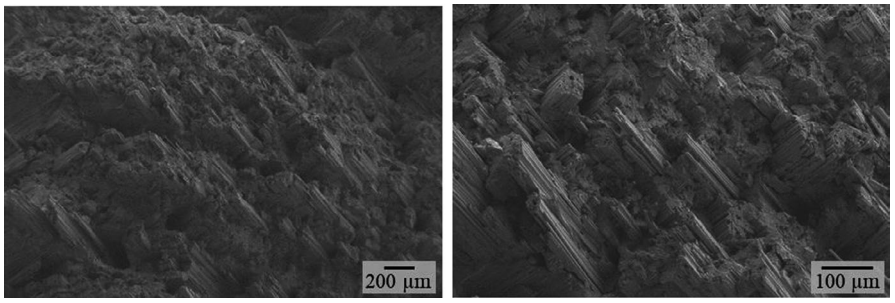

FIGURE 15 Fracture surface of C/C-SiC with fiber orientation ±30° resembling a rather low fiber pull-out (magn. 100× [left] and 350× [right])

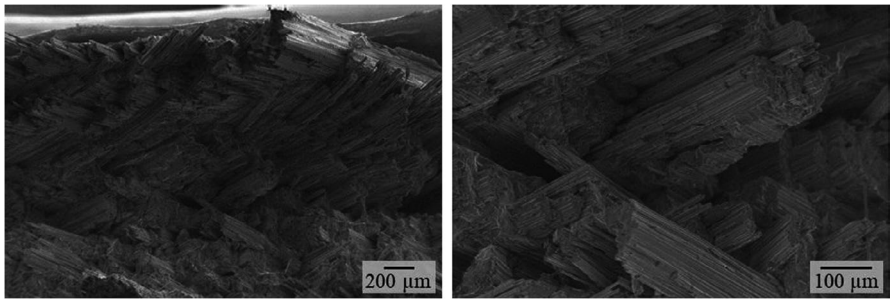

FIGURE 16 Fracture surface of C/C-SiC with fiber orientation ±45° resembling fiber pull-out and matrix disintegration (magn. 100× [left] and 350× [right])

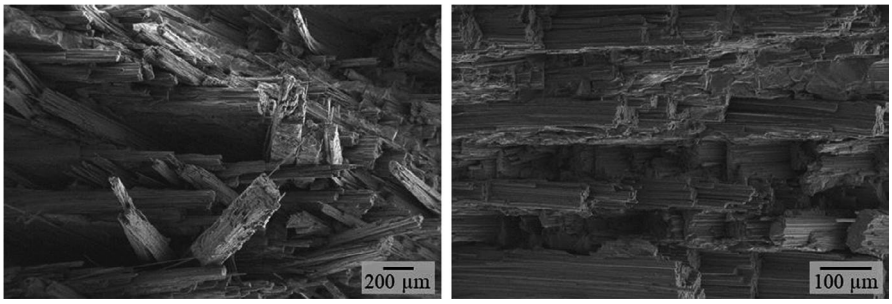

FIGURE 17 Fracture surface of C/C-SiC with fiber orientation ±60° resembling fiber pull-out and rather high matrix disintegration (magn. 100× [left] and 350× [right])

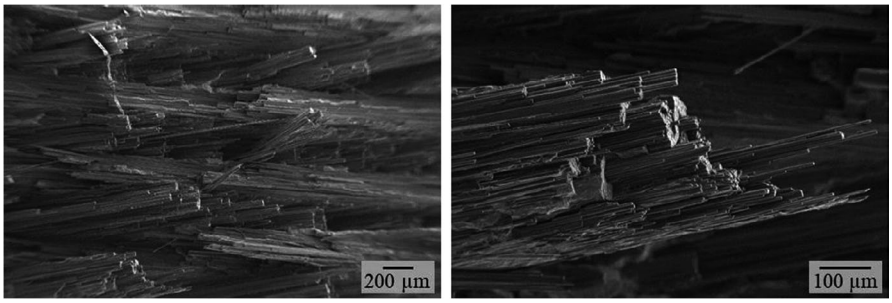

FIGURE 18 Fracture surface of C/C-SiC with fiber orientation ±75° resembling high amount of matrix disintegration; almost no matrix is visible anymore (magn. 100× [left] and 350× [right])

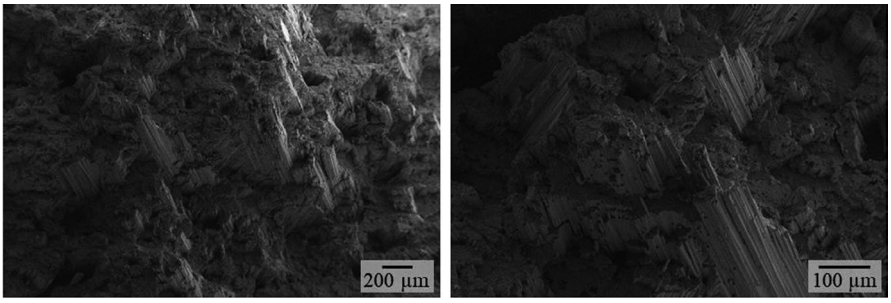

FIGURE 19 Fracture surface of C/C-SiC with fiber orientation ±15° after being tested at 1,300°C resembling a rather high fiber pull-out. But the amount of fiber pull-out seems to be slightly lower compared to the samples tested at room temperature (see Figure 14) (magn. 100× [left] and 350× [right])

can be achieved by water-cooled copper tubes such that multiple test runs can be performed within one day.

3 | RESULTS AND DISCUSSION

3.1 | Mechanical properties, density, and open porosity of C/C-SiC composite plates at room temperature

In Table 1, the mechanical properties, density, and open porosity of C/C-SiC composite plates are listed for various fiber orientations ranging from ±15° to ±75°. Whereas the winding angle has only minor influence on density and open porosity of composite plates (CFRP, C/C and C/C-SiC), there is a big influence on tensile strength and modulus as well as fracture strain in C/C-SiC state. Tensile strength versus fiber orientation is shown in Figure 4, revealing asymptotic behavior: the highest tensile strength is at the lowest fiber orientation, meaning that the main fiber direction is oriented in tensile loading direction (Figures 5 and 6). Furthermore, a graphical illustration of the tensile behavior of C/C-SiC tested at room temperature as well as high temperature (1,300°C) versus fiber orientation is shown in Figure 13.

3.2 | Microstructure of C/C-SiC composite plates at room temperature

The microstructure of C/C-SiC composite plates obtained by wet filament winding and LSI-processing in dependence on the winding angle is shown in Figures 7–9.

3.3 | Thermomechanical properties of C/C-SiC composite plates at high temperature (1300°C)

In Table 2, the thermomechanical properties of C/C-SiC composite plates are listed for various fiber orientations ranging from ±15° to ±75° (Figures 10–12). Furthermore,

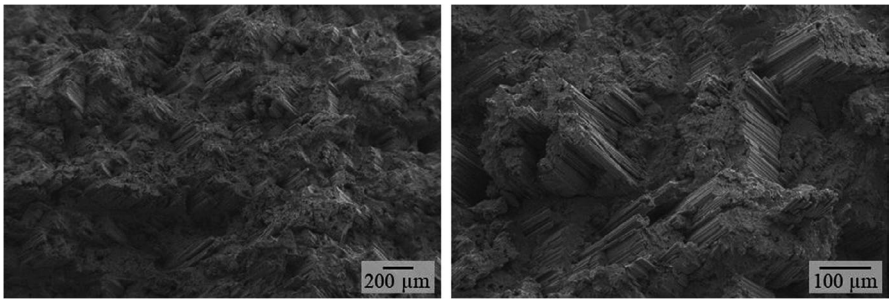

FIGURE 20 Fracture surface of C/C-SiC with fiber orientation ±30° after being tested at 1,300°C resembling a rather low fiber pull-out (magn. 100× [left] and 350× [right])

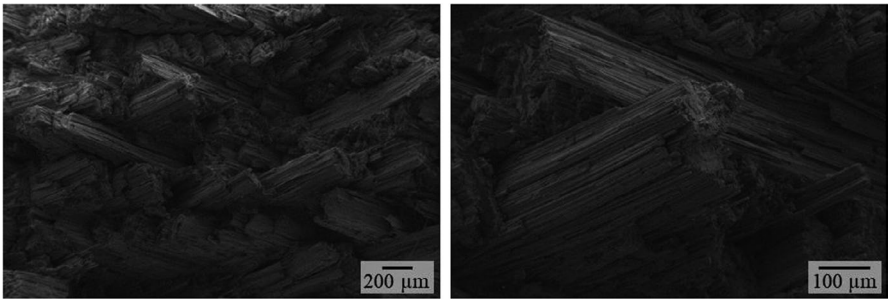

FIGURE 21 Fracture surface of C/C-SiC with fiber orientation ±45° after being tested at 1,300°C resembling a rather low fiber pull-out and matrix disintegration; almost no matrix is visible anymore (magn. 100× [left] and 350× [right])

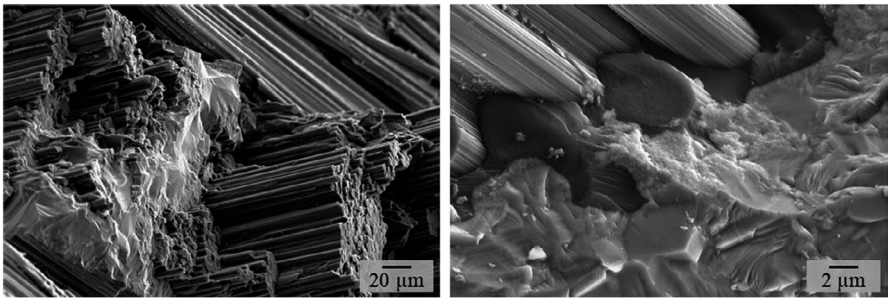

FIGURE 22 Magnified fracture surface of C/C-SiC with fiber orientation ±45° after being tested at 1,300°C resembling a rather low fiber pull-out and matrix disintegration; no coating is visible (magn. 1,000× [left] and 10,000× [right])

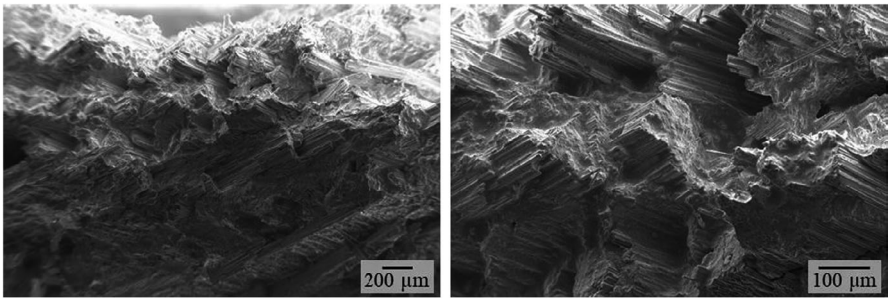

FIGURE 23 Fracture surface of C/C-SiC with fiber orientation ±45° after being tested at 1,600°C resembling a rather low fiber pull-out and rather brittle failure (magn. 100× [left] and 350× [right])

a graphical illustration of the tensile behavior of C/C-SiC tested at room temperature as well as high temperature (1300°C) versus fiber orientation is shown in Figure 13.

It is interesting to note that for a fiber orientation of ±15° tensile strength of filament wound C/C-SiC at high temperature (1300°C) is about 10% higher than at room temperature. This effect is more pronounced at a fiber orientation of ±30° (+28%) and even more at ±45° (+47%). Similar to this finding is the behavior of the C/C-SiC composite with respect to stiffness. If the fibers are predominately oriented in loading direction (±15° and ±30°), the stiffness is increased with testing temperature since C-fibers are more and more stretched with temperature due to the alpha mismatch with the SiC matrix with much higher thermal expansion. The fibers dominate the stiffness of the composite because the SiC matrix is permeated with small cracks. At a fiber orientation of ±45°, this effect is negligible since the stiffness of the C-fibers, due to the low contribution in loading direction, cannot contribute to the stiffness of the composite any more.

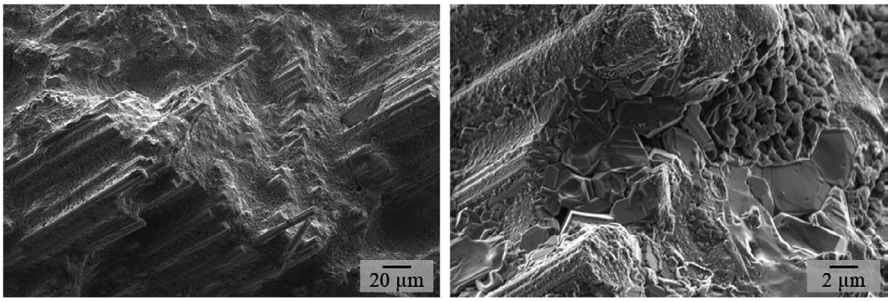

FIGURE 24 Magnified fracture surface of C/C-SiC with fiber orientation ±45° after being tested at 1,600°C resembling a rather low fiber pull-out and rather brittle failure. Note that C-fibers and C-matrix are covered with a thin structured coating, presumably SiC (magn. 1,000× [left] and 10,000× [right])

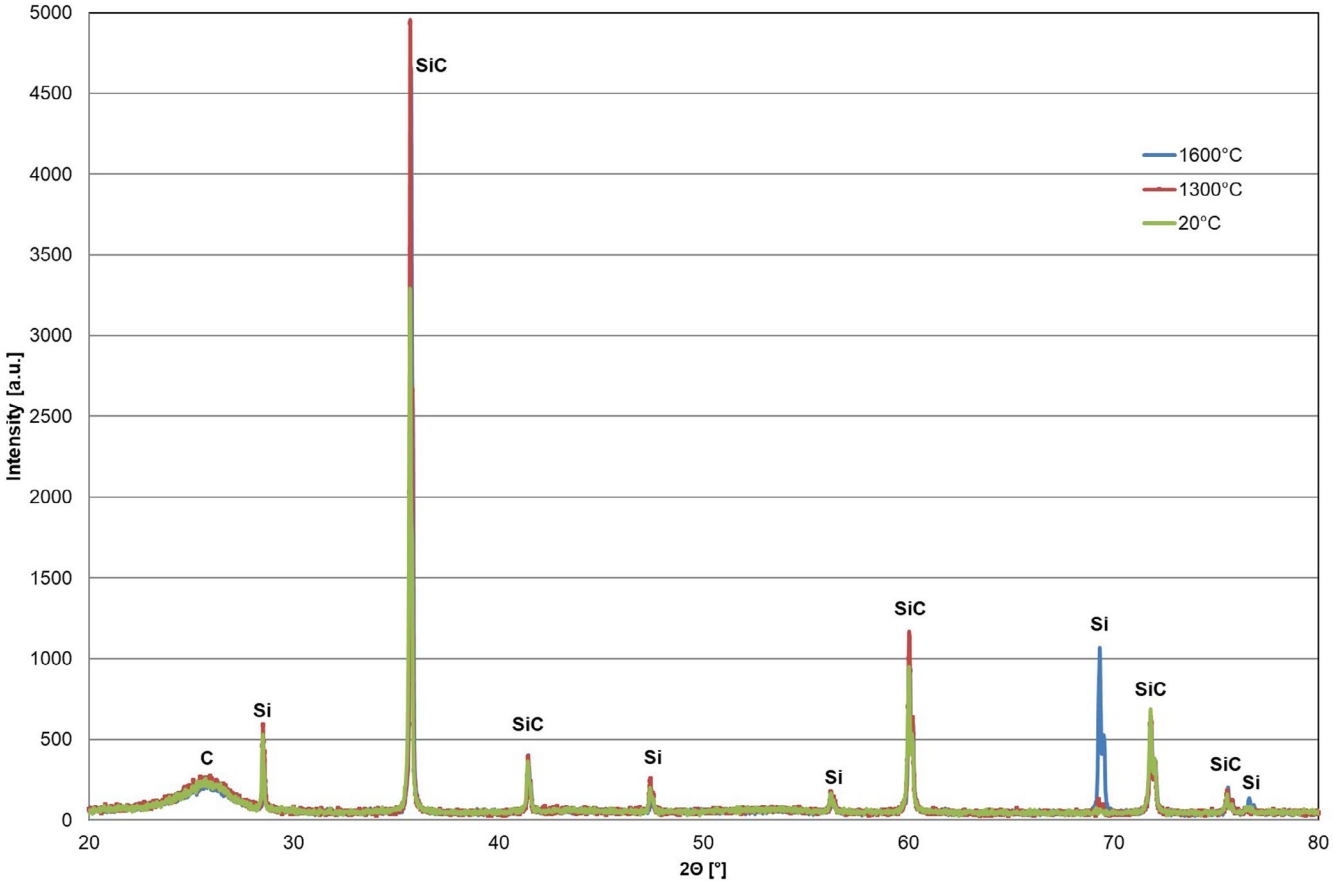

FIGURE 25 XRD-diffractograms of C/C-SiC with fiber orientation ±45° after being tested at 1600°C (blue), 1300°C (red), and original C/C-SiC (green) with same fiber orientation. Peak heights of C and SiC were kept constant, since their main amounts are predetermined by LSI processing and only the small amount of Si (typically in the range of 1%–2%) is sensitive to significant changes by gas phase processes

3.4 | Fracture surface images of C/C-SiC composite coupons at room temperature

The fractured surfaces were analyzed by SEM by tilting the fractured surfaces out of the *xz* plane for better visibility (Figures 14–18). It seems that the lower the winding angle is, the more fiber pull-out and appearance of matrix can be observed.

3.5 | Fracture surface of C/C-SiC composite coupons at high temperature (1300°C)

In Figures 19–22, the fractured surfaces of C/C-SiC composite specimens tested at 1,300°C are shown. It seems that the lower the winding angle is the more fiber pull-out and appearance of matrix can be observed. In Figure 22, details of the applied C-fiber (T800) are shown: potato-shaped cross section

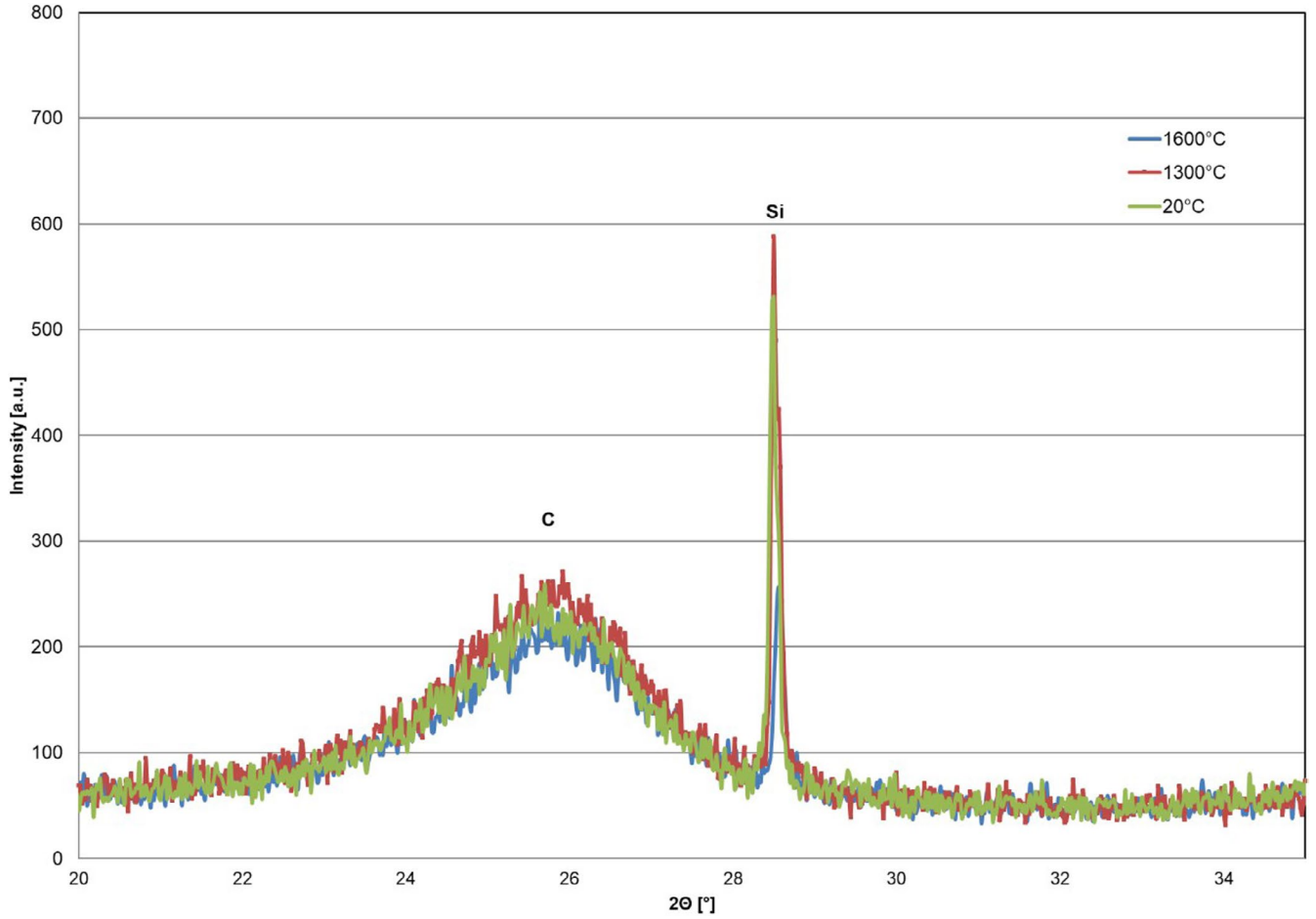

FIGURE 26 Enlarged section of XRD-diffractograms of C/C-SiC with fiber orientation ±45° after being tested at 1600°C (blue), 1300°C (red), and original C/C-SiC (green) with same fiber orientation. Peak heights of C and SiC were kept constant, since their main amounts are predetermined by LSI processing and only the small amount of Si (typically in the range of 1%–2%) is sensitive to significant changes by gas phase processes. Note that the Si peak of C/C-SiC tested at 1600°C (blue) is about one third in height compared to the other two samples

with a fairly rough structured surface without visible coatings, whereas Figure 24 does not show these details since it is covered by a presumably SiC coating convoluting those details.

3.6 | Fracture surface of C/C-SiC composite coupons at high temperature (1600°C)

In Figures 23 and 24, the fractured surface of a C/C-SiC specimen tested at 1600°C is shown. Due to the fact that the marking color painted on C/C-SiC did not survive these harsh conditions (1600°C, 1 mbar N_2, C, and liquid Si as potential reactants), we were not able to determine the fracture strain and thus not the tensile modulus either. As a rough estimate for tensile strength, a value of 92 MPa could be obtained. However, further measurements with a superior marking color must be performed in the near future.

Furthermore, it should be noticed that the partial pressure of gaseous silicon at 1600°C is increased by a factor of more than 100 compared to the case at 1300°C. In addition, the reaction rate of SiC-formation on the surface of carbon with gaseous silicon is also depending on the partial pressure of silicon resulting in a 10 000-fold increase in the reactivity of excess silicon to form SiC on carbon surfaces (C-fibers and C-matrix, and not to forget C-susceptor). This finding could not be detected on the surface of the sample tested at 1300°C (Figure 22); however, it was observed on the surface of the sample tested at 1600°C at a pressure of 1 mbar (Figure 24) and in XRD-investigations (Figures 25 and 26), where the Si-peak at 2θ equals about 28.4°, typically assigned to 1–2 wt% Si of the composite. Exactly that peak, clearly visible at neat samples and specimens tested at 1,300°C, diminishes rapidly to specimens tested at 1,600°C. This finding could explain a possible decrease in tensile strength with testing temperature as well as the diminishing of the markings. Therefore, further high-temperature testing is mandatory.

In addition, the testing conditions should be adapted based on these findings:

- High-temperature testing (>1300°C) in Ar-atmosphere at ambient pressure (1 bar) in order to minimize Si gas formation and reaction with carbon via gas phase reactions.

- High-temperature testing in N_2-atmosphere should be avoided due to silicon nitride and possible whisker formation.
- High-temperature testing with suitable markings in order to be able to evaluate strain to failure via laser extensometer and tensile modulus by suitable calculations.

4 | CONCLUSION

It was shown in this paper that the manufacture of C/C-SiC composite materials by wet filament winding of C-fibers with a water-based phenolic resin with subsequent curing via autoclave as well as pyrolysis and liquid siliconisation is feasible and reproducible. Almost dense C/C-SiC composite materials with different winding angles ranging from ±15° to ±75° could be obtained with porosities lower than 3% and densities in the range of 2 g/cm^3. Thermomechanical characterization via tensile testing at room temperature and at 1300°C revealed higher tensile strength at elevated temperature than at room temperature. Crack patterns during pyrolysis, microstructure after siliconisation, and tensile strength strongly depend on the fiber/matrix interface strength and winding angle. Moreover, calculation tools for composites, such as classical laminate and inverse laminate theory, can be applied for structural evaluation, design, and prediction of mechanical performance of C/C-SiC structures. Thus, C/C-SiC material obtained by wet filament winding and LSI-processing has excellent high temperature strength for high-temperature applications.

ACKNOWLEDGMENT

Financial support by the German Ministry of Defence (BAAINBw) is gratefully acknowledged.

ORCID

Martin Frieß https://orcid.org/0000-0002-4425-8244
Fabia Süß https://orcid.org/0000-0002-5016-5781
Yuan Shi https://orcid.org/0000-0002-4210-9069

REFERENCES

1. Jamet JF, Lamicq PJ. In: Naslain R, editor. High-Temperature Ceramic Matrix Composites. London: Woodhead; 1993. p. 735.
2. Krenkel W. Carbon fiber reinforced CMC for high performance structures. Int J Appl Ceram Technol. 2004;1:188–200.
3. Naslain R. Design, preparation and properties of non-oxide CMCs for application in engines and nuclear reactors: an overview. Comp Sci Technol. 2004;64:155–70.
4. Krenkel W, Kochendörfer R. The LSI process: a cost effective processing technique for ceramic matrix composites. Proc Int Conf on Adv Mater. 1996.
5. Fabig J, Krenkel W. Principles and new aspects in LSI-processing. Adv Sci Technol. 1999;22:141–8.
6. Frieß M, Renz R, Krenkel W. Advanced inorganic structural fiber composites IV. Adv Sci Technol. 2002;40:141.
7. Frieß M, Krenkel W, Kochendörfer R, Brand R, Neuer G, Maier H-P. in Basic research and technology for two-stage-to-orbit vehicles. Weinheim: Wiley-VCh; 2005. ISBN 3-527-27735-8.
8. Stahl V, Shi Y, Kraft W, Lanz T, Vetter P, Jemmali R, et al. C/C-SiC component for metallic phase change materials. Int J Appl Ceram Technol. 2020;17(5):2040–205.
9. Ding W, Shi Y, Kessel F, Koch D, Bauer T. Characterization of corrosion resistance of C/C–SiC composite in molten chloride mixture $MgCl_2$/NaCl/KCl at 700 °C. npj Materials Degradation. 2019;3(1)
10. Hald H, Weihs H, Reimer T. Proceedings of the 53rd International Astronautical Congress, Houston/Texas, USA. 2002.
11. Frieß M, Zuber C, Hofmann S, Crippa M, Heidenreich B. Verbundwerkstoffe und Werkstoffverbunde. Weinheim: Wiley-VCh; 2009. p. 257.
12. Frieß M, Scheiffele M, Zankl W, Hofmann F. Development, manufacture and characterization of C/C-SiC components based on filament winding. In Proc. 7th Int. Conf. on High Temp. Ceram. Matrix Comp. HT-CMC7, 2010.
13. Breede F, Klatt E, Frieß M, Voggenreiter H. Mechanical properties and microstructures of C/C-SiC composite plates by wet filament winding technique. In Proc. 7th Int. Conf. on High Temp. Ceram. Matrix Comp. HT-CMC7, 2010.
14. Reimer T, Petkov I, Koch D, Frieß M, Dellin C. Fabrication and characterization of C/C-SiC material made with pitch-based carbon fibres. Ceram Transact. 2015;252. https://doi.org/10.1002/9781119183860.ch28
15. Krenkel W. Entwicklung eines kostengünstigen Verfahrens zur Herstellung von Bauteilen aus keramischen Verbundwerkstoffen. Dissertation Uni Stuttgart. 2000.
16. Krenkel W, Hausherr J, Frieß M, Reimer T. Design, Manufacture and Quality Assurance of C/C-SiC Composites for Aeronautics and Space Transportation Systems. 28th International Cocoa Beach Conference and Exposition on Advanced Ceramics & Composites, Cocoa Beach, Florida, USA, 25-30.01.2004, The American Ceramic Society; 2004.
17. Heidenreich B, Zuber C, Rheinwald C, Benitsch B. C/C-SiC materials with unidirectional reinforcement. In Proc. 6th Int. Conf. on High Temp. Ceram. Matrix Comp. HT-CMC6; 2007.
18. Heidenreich B, Hofmann S, Jemmali R, Frieß M, Koch D. C/C-SiC materials based on melt infiltration – manufacturing methods and experiences from serial production. HT-CMC 8, Xi'an China Sept.; 2013.
19. Brandt R, Frieß M, Neuer G. Thermal conductivity, specific heat capacity, and emissivity of ceramic matrix composites at high temperatures. High Temp High Press. 2003;35:169–77.
20. Shi Y, Kessel F, Frieß M, Jain N, Tushtev K. Characterization and modeling of tensile properties of continuous fiber reinforced C/C-SiC composite at high temperatures. J Eur Ceram Soc. 2020;41(5):3061–71.
21. Shi Y, Xiu Y, Koch D. Investigation of statistical distribution of C/C-SiC composite's mechanical properties. Key Eng Mater. 2019;809:131–9.
22. Shi Y, Neubrand A, Koch D. Characterization of hardness and stiffness of ceramic matrix composites through instrumented indentation test. Adv Eng Mater. 2018;21:1800806.

How to cite this article: Frieß M, Böyükbas M, Vogel F, et al. Manufacture and thermomechanical characterization of wet filament wound C/C-SiC composites. *Int J Appl Ceram Technol*. 2022;19:34–44. https://doi.org/10.1111/ijac.13785